Chemical-looping combustion and chemical-looping reforming in a circulating fluidized-bed reactor using Ni-based oxygen carriers

Magnus Rydén*, Anders Lyngfelt, Tobias Mattisson
Department of Energy and Environment
Chalmers University of Technology
SE-412 96, Göteborg, Sweden

Abstract

Three oxygen carriers for chemical-looping combustion and chemical-looping reforming have been investigated in a small circulating fluidized-bed reactor. N2AM1400 was produced by freeze granulation with $MgAl_2O_4$ as support material and had a NiO content of 20%. Ni18-αAl was produced by impregnation onto α-Al_2O_3 and had a NiO content of 18%. Ni21-γAl was produced by impregnation onto γ-Al_2O_3 and had a NiO content of 21%. Over 160 hours of operation has been recorded. The conversion of natural gas into products was 96-100% depending on oxygen carrier and experimental conditions. For chemical-looping combustion, N2AM1400 and Ni21-γAl provided poor selectivity towards CO_2 and H_2O while Ni18-αAl initially showed very high selectivity, which declined as a function of time. For chemical-looping reforming, operating the reactor at the desired process parameters, which was a fuel reactor temperature of 950ºC and an air factor of 0.30, was possible with all of the tested oxygen-carrier materials. When only natural gas was used as fuel, there was significant formation of solid carbon in the fuel reactor for Ni18-αAl and Ni21-γAl. Adding 30% steam or CO_2 to the fuel removed or decreased the carbon formation. During the course of the experiments, N2AM1400 and Ni18-αAl retained their physical and chemical structure, while Ni21-γAl displayed a significant reduction in porosity but remained highly reactive.

Keywords: Chemical-Looping Combustion; Chemical-Looping Reforming; Partial Oxidation; Auto-Thermal Reforming; Hydrogen; Synthesis Gas.

---

*Corresponding author: Tel. (+46) 31 7721457, Email: magnus.ryden@chalmers.se
Energy & Fuels 2008; 22: 2585–2597.

1. Introduction

In later years, concerns that emissions of CO_2 from combustion of fossil fuels may lead to changes in the climate of the earth have been growing steadily. A majority of the scientific community now concludes that global CO_2 emissions would need to be reduced greatly in the future.

One way to reduce CO_2 emissions that is receiving increasing interest is CO_2 sequestration, which is the capture of CO_2 in an emission source and storing it where it is prevented from reaching the atmosphere. This could involve for example CO_2 capture in flue gases from combustion processes, and CO_2 storage in geological formations such as depleted oil and gas fields or deep saline aquifers. Carbon sequestration has potential to greatly reduce CO_2 emissions from large point sources such as power plants and industries.

In contrast, CO_2-capture applications for small mobile emission sources such as cars, trucks and airplanes seem implausible. This is noteworthy since the transportation sector is responsible for considerable share of the global CO_2 emissions. Most likely, CO_2 capture would also be complicated and expensive for small-scale applications due to unfavourable economics of scale.

There are ways to address this dilemma. It is well established that fossil fuels can be converted into H_2 via various reforming processes. If CO_2 is captured within the reforming process, produced H_2 could be used as a CO_2-free fuel for vehicles, as well as for or other applications. H_2 is a versatile energy carrier that can be burnt in combustion engines or gas turbines, and is also the ideal fuel for most types of fuel cells.

The chemical-looping concept involves oxidation of a fuel using oxygen from a solid oxygen carrier instead of oxygen from air. This way the products are not diluted with N_2. This is an interesting concept both for CO_2 capture applications in combustion processes and for H_2 generation through reforming processes. Hence chemical looping is a technology that may have a significant role to play in the global task to reduce anthropogenic CO_2 emissions.

2. Technical background

2.1 Chemical-looping combustion

Chemical-looping combustion is an innovative combustion technology that can be used for CO_2 capture in power generating processes. Two separate reactors are used, one for air and one for fuel. A solid oxygen carrier performs the task of transporting oxygen between the reactors. Hence direct contact between fuel and air is avoided and the combustion products are not diluted with N_2, see Figure 1.

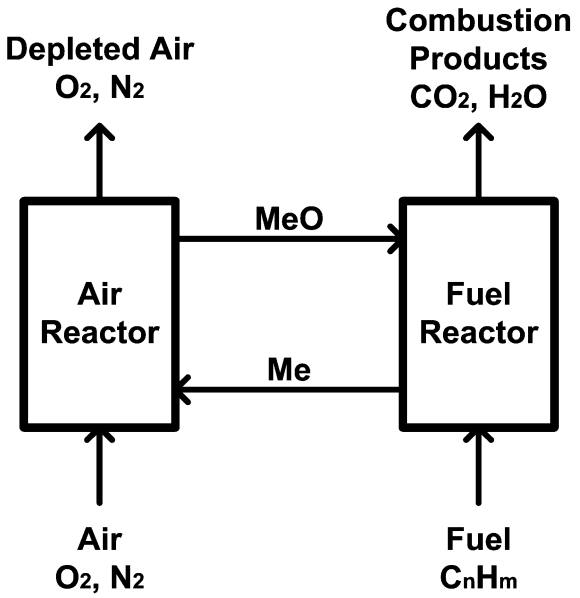

Figure 1. Schematic description of chemical-looping combustion.

Typically, the abbreviation MeO is used to describe the oxygen carrier in its oxidized form, while Me is used for the reduced form. This is because many potential oxygen-carrier materials are metal oxides, for example NiO, Fe_2O_3, Mn_3O_4 and CuO.

The oxygen carrier circulates between the reactors. In the fuel reactor, it is reduced by the fuel, which in turn is oxidized to CO_2 and H_2O according to reaction (1). In the air reactor, it is oxidized to its initial state with O_2 from the combustion air according to reaction (2).

$$C_nH_m + (2n+½m)\ MeO \rightarrow n\ CO_2 + ½m\ H_2O + (2n+½m)\ Me \quad (1)$$

$$Me + ½\ O_2 \rightarrow MeO \quad (2)$$

The amount of energy released or required in each reactor vessel depends on the nature of the oxygen carrier and the fuel. Reaction (2) is always strongly exothermic. For most oxygen-carrier materials, reaction (1) is endothermic if the fuel is a hydrocarbon. If CO or H_2 is used as fuel or if CuO is used as oxygen carrier, reaction (1) is slightly exothermic. If reaction (1) is endothermic the flow of solid oxygen carrier can be used to transport sensible heat from the air reactor to the fuel reactor. The net energy released in the reactor system is the same as for ordinary combustion. This is apparent since combining reaction (1) and reaction (2) yields reaction (3), which is complete combustion of the fuel with O_2.

$$C_nH_m + (n+¼m)\ O_2 \rightarrow n\ CO_2 + ½m\ H_2O \qquad (3)$$

Compared with conventional combustion, chemical-looping combustion has several potential benefits. The exhaust gas from the air reactor is harmless, consisting mainly of N_2 and possibly some O_2. There should be no thermal formation of NO_X since regeneration of the oxygen carrier takes place without flame and at moderate temperatures. The gas from the fuel reactor consists of CO_2 and H_2O, and cooling in a condenser is all that is needed to obtain almost pure CO_2.

Possible side reactions include formation of solid carbon in the fuel reactor. This is unwanted since solid carbon could follow the oxygen-carrier particles to the air reactor and burn there, which would reduce the degree of CO_2 capture. Solid carbon could be formed either through the Boudouard reaction, reaction (4), or through hydrocarbon decomposition, reaction (5). Formation of solid carbon is well documented from various chemical processes, and it is well established that reactions (4-5) can be catalysed by metallic surfaces.

$$2\ CO \rightarrow C + CO_2 \qquad (4)$$

$$C_nH_m \rightarrow n\ C + ½m\ H_2 \qquad (5)$$

In practice, a chemical-looping combustion process could be designed in different ways, but circulating fluidized beds with oxygen-carrier particles used as bed material are likely to have an advantage over other alternatives since this design is straightforward, provides good contact between gas and solids and allows a smooth flow of oxygen carrier between the reactors.

In later years, when carbon sequestration has become a widely discussed issue, the interest for chemical-looping combustion has grown. The research has focused on experimental and theoretical investigations of possible oxygen-carriers and on process studies examining how chemical-looping combustion could be used for power generation. A feasible oxygen-carrier material for chemical-looping combustion should:

- Have high reactivity with fuel and oxygen.
- Be thermodynamically capable to convert a large share of the fuel to CO_2 and H_2O.
- Have a sufficiently high oxygen ratio, e.g. the weight fraction of the material that is oxygen which can react according to reaction (1) should be high.
- Have low tendency towards fragmentation, attrition, agglomeration and other kinds of mechanical or thermal degeneration.
- Not promote extensive formation of solid carbon in the fuel reactor.
- Be cheap and preferably environmentally sound.

At present, metal oxides such as NiO, Fe_2O_3, Mn_3O_4 and CuO supported on inert carrier material such as Al_2O_3 or ZrO_2 seem like the most likely candidates to meet those criteria. An overview of the research treating these kinds of oxygen-carriers can be found in the works of Cho[1], Johansson[2] and Adánez et al[3]. Information about additional potential oxygen-carrier materials can be found in the work of Jerndal et al[4], which includes a theoretical examination of 27 different oxide systems. Carbon formation on oxygen-carrier particles for chemical-looping combustion has been specifically examined for example by Cho et al[5]. Continuous chemical-looping combustion in circulating fluidized beds has been demonstrated by Lyngfelt et al[6], Ryu et al[7], Johansson et al[8,9], Abad et al[10,11], Adánez et al[12], Linderholm et al[13] and De Diego et al[14]. Reaction kinetics for oxygen carriers based on NiO, Fe_2O_3 and CuO have been examined by Abad et al[15,16]. The effects of pressure on the properties of various oxygen-carrier materials have been examined by García-Labiano et al[17]. An overview of various subjects regarding chemical-looping combustion, such as design of experimental reactors, power production with CO_2 capture and more about oxygen-carriers can be found in the doctoral theses by Brandvoll[18], Johansson[19], Wolf[20], Kronberger[21] and Naqvi[22].

2.2 Chemical-Looping Reforming

Chemical-looping reforming, as described in this paper, was proposed in 2001 by Mattisson et al[23]. The idea is older though. Conrad Arnold representing the Standard Oil Development Company was granted a patent of a process similar to chemical-looping reforming as early as 1950[24].

Chemical-looping reforming utilizes the same basic principles as chemical-looping combustion. The difference is that the products desired are not heat but synthesis gas, a mix of H_2 and CO. Therefore the air to fuel ratio is kept low to prevent the fuel from becoming fully oxidized to CO_2 and H_2O. Chemical-looping reforming in its most basic form could be described as a process for partial oxidation of hydrocarbon fuels, where a solid oxygen carrier is used as a source of undiluted oxygen. This is favourable since it would eliminate the need for expensive and power demanding air separation. The basic principles of chemical-looping reforming are illustrated in Figure 2.

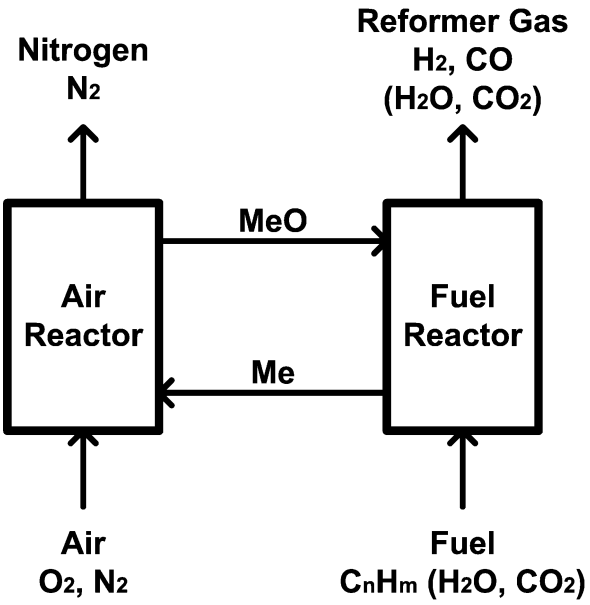

Figure 2. Schematic description of chemical-looping reforming.

In the air reactor, reaction (2) will occur, just as in chemical-looping combustion. In the fuel reactor, some fuel may become completely oxidized to CO_2 and H_2O via reaction (1), but a large share should react according to reaction (6), partial oxidation using oxygen from the oxygen carrier.

$$C_nH_m + n\ MeO \rightarrow n\ CO + \tfrac{1}{2}m\ H_2 + n\ Me \quad (6)$$

Steam or CO_2 could be added to the fuel to enhance the relative importance of steam reforming, reaction (7), or CO_2 reforming, reaction (8), respectively. This could be useful if synthesis gas with a H_2/CO ratio that does not correspond to the H/C ratio of the fuel is desired.

$$C_nH_m + n\ H_2O \leftrightarrow n\ CO + (n + \tfrac{1}{2}m)\ H_2 \quad (7)$$

$$C_nH_m + n\ CO_2 \leftrightarrow 2n\ CO + \tfrac{1}{2}m\ H_2 \quad (8)$$

The overall reaction energy of the reactor system varies as the relative importance between reactions (1-2) and reactions (6-8) is altered. When the fuel and oxygen carrier reacts according to reactions (1) and (2), heat corresponding to the lower heating value of the fuel is released. When the fuel reacts according to reactions (6) and (2), heat corresponding to the reaction energy for partial oxidation of the fuel is released. Reactions (7-8) are strongly endothermic and do not provide any reduced oxygen carrier to be reoxidized with the exothermic reaction (2). A thermo neutral reactor system is desirable since external heating at relevant temperatures would be unfavourable from a technical point of view. Therefore, steam reforming and CO_2 reforming can not be allowed to dominate the process since this would make the reactor system endothermic.

The outlet from the fuel reactor consists of H_2, H_2O, CO and CO_2, and could be used as feedstock for chemical processes or for production of H_2, just as synthesis gas from other reforming or partial oxidation processes. Due to reaction kinetics and thermodynamics it is possible that there will be some unreformed CH_4 in the reformer gas if the reactor temperature is not sufficiently high. If thermodynamic equilibrium is assumed, a fuel reactor temperature in the order of 800ºC should be sufficient to achieve at least 99% conversion of CH_4 at atmospheric pressure. At elevated pressure, somewhat higher temperature may be necessary due to less favourable thermodynamics.

If H_2 is the desired product, the fuel reactor gas would need to undergo water-gas shift, reaction (9), which is a slightly exothermic reaction that takes place in a separate reactor at temperatures between 200ºC and 500ºC.

$$CO + H_2O \leftrightarrow CO_2 + H_2 \quad (9)$$

Oxygen-carrier materials for chemical-looping reforming would need to have about the same properties as those for chemical-looping combustion. The main difference is that they must be capable to convert the fuel to CO and H_2 when the air to fuel ratio is reduced, rather than produce CO_2, H_2O and unreformed fuel.

Oxygen carriers for chemical-looping reforming have been examined by Zafar et al[25], who performed tests in a fluidized-bed reactor with oxygen-carrier particles as fluidizing agent, and by Mattisson et al[26]. These two studies indicate high reaction rate and good selectivity towards H_2 and CO for oxygen carriers with NiO as active phase, while oxygen carriers based on Fe_2O_3, Mn_3O_4 and CuO suffered from poor selectivity and produced mostly CO_2, H_2O and unreformed CH_4. Continuously operating chemical-looping reforming in a circulating-fluidized bed reactor system has been demonstrated by Rydén et al[27,28], who found that chemical-looping reforming of natural gas with an oxygen-carrier consisting of 60% NiO supported on $MgAl_2O_4$ was feasible, but that carbon formation could be an obstacle unless the fuel was mixed with some steam. An overview of various subjects regarding chemical-looping reforming can be found in the licentiate thesis by Rydén[28].

In later years, other process concepts sharing attributes with chemical-looping reforming have also been proposed. Stobbe et al[29] have suggested a process involving oxidation and reduction of manganese oxide. Fathi et al[30], Gavalas et al[31] and Jalibert et al[32] have suggested and examined partial oxidation of CH_4 by oxidation and reduction of CeO_2 promoted with various catalysts. Shen et al[33, 34], Zeng et al[35], Li et al[36], Bjørgum[37] and Rydén et al[38] have studied the possibility to generate synthesis gas by cyclic oxidation and reduction of perovskites such as $La_xSr_{1-x}Fe_yCo_{1-y}O_{3-\delta}$, in similar fashion as is done in chemical-looping reforming.

2.3 The aim of this study

The main objective with this study is to show that the chemical-looping reforming concept is feasible, i.e. that high conversion of fuel into H_2 and CO can be achieved at air factors close to stoichiometric partial oxidation, and that carbon formation can be reduced by adding some H_2O to the fuel. In addition to this, the general characteristics of three potential oxygen-carrier materials for chemical-looping applications have been examined.

3. Experimental

3.1 The reactor system

The experiments were carried out in a small-scale laboratory reactor. The reactor is an improved and slightly altered version of a fluidized-bed reactor that has been used for continuously operating chemical-looping experiments by various authors[8,9,10,11,19,27,28]. A schematic picture is shown in Figure 3.

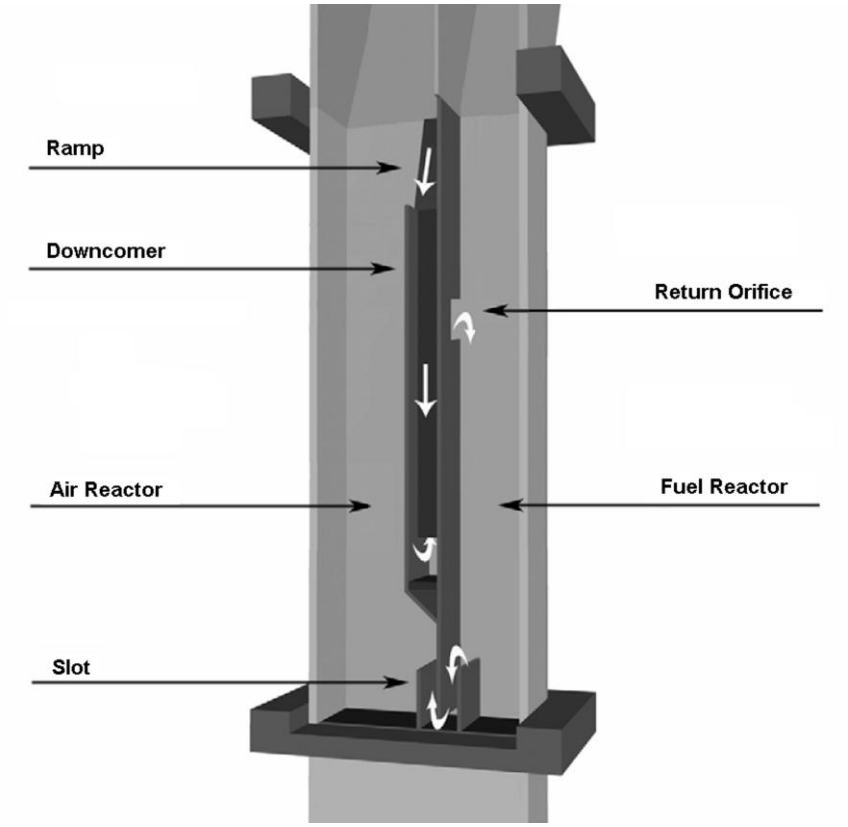

Figure 3. Schematic description of the reactor.

The reactor is designed for chemical-looping combustion experiments using gaseous fuels. Suitable flows are 0.20-0.75 L_n/min natural gas and 3-10 L_n/min air. Chemical-looping reforming experiments can be performed by increasing the natural-gas flow to 0.9-1.6 L_n/min, while using a suitable air flow.

The reactor is 200 mm high. The base of the fuel reactor measures 25×25 mm. The air reactor is 25×40 mm in the bottom and 25×25 mm in the upper narrow part. Fuel and air enter the system through separate wind boxes, located in the bottom of the reactor. Porous

quartz plates act as gas distributors. In the air reactor the gas velocity is sufficiently high for oxygen-carrier particles to be thrown upwards. A fraction of these particles falls into the downcomer, which is a J-type loop-seal. From the loop-seal, particles are ejected into the fuel reactor via the return orifice. Particles returns the air reactor through a slot situated in the bottom of the wall between the reactor sections. In this way, a continuous circulation of oxygen-carrier particles is obtained. The downcomer and the slot are fluidized with small amounts of inert N_2.

Above the reactor there is a separate vessel for particle separation. Here, the reactor widens to decrease the gas velocity and allow particles to fall back into the reactor beds. The particle separation part is 240 mm high, and in the first 180 mm the reactor depth expands from 25 mm to 105 mm. The last 60 mm has a constant cross-section area. The particles falling down in the sloping section above the air reactor are led to the downcomer by a leaning wall.

The slot has two walls rising from the bottom plate, separated by 10 mm. The wall at the air reactor half is 20 mm and slightly curved, while the wall at the fuel reactor half is 15 mm. The wall that separates the fuel and air reactor is situated between these two walls and stops 12 mm above the bottom plate. Fluidization gas is added via a horizontal pipe with three 1-mm holes directed downwards.

In order to make it possible to reach and sustain a suitable temperature, the whole reactor is placed inside an electrically heated furnace. The temperature of the furnace is controlled with thermocouples located inside the furnace, just outside the reactor. The temperature in each reactor section is measured with thermocouples located 70 mm above the distributor plates.

On the exit pipe from the fuel reactor there is a water seal that makes it possible to increase the pressure in the fuel reactor by altering the height of the water column. This is done in order to prevent dilution of the fuel reactor gas with leaking air from the air reactor.

Along the reactor sections there are thirteen separate pressure measuring taps. By measuring pressure differences, it is possible to estimate the distribution of solids within the system, and to detect problems such as defluidization.

3.2 Fuel

Natural gas with a composition equivalent to $C_{1.14}H_{4.25}O_{0.01}N_{0.005}$ was used as fuel. The composition is given in Table 1.

Component		x_i (%)
Methane	CH_4	89.80
Ethane	C_2H_6	5.82
Propane	C_3H_8	2.31
I-butane	C_4H_{10}	0.39
N-butane	C_4H_{10}	0.53
I-pentane	C_5H_{12}	0.12
N-pentane	C_5H_{12}	0.08
Hexane +	C_6+	0.06
Nitrogen	N_2	0.27
Carbon Dioxide	CO_2	0.62

Table 1. Composition of the natural gas.

Steam could be added to the fuel by bubbling it through hot water with a temperature of 90ºC. The steam-rich gas mixture was cooled to the desirable saturation temperature in a cooling column and transferred to the reactor in a heated tube with a temperature of 150ºC. If desired, it was also possible to dilute the fuel with CO_2 or N_2.

3.3 Oxygen-carrier materials

Three nickel-based oxygen carriers have been examined, see Table 2. The fraction of NiO in each material is expressed by weight.

Oxygen carrier	Chemical composition	Production method	Size (µm)	Porosity (%)	Solids inventory (g)
N2AM1400	20% NiO on $MgAl_2O_4$	Freeze granulation	90-212	35	250
Ni18-αAl	18% NiO on α-Al_2O_3	Impregnation	90-212	53	180-250
Ni21-γAl	21% NiO on γ-Al_2O_3	Impregnation	90-250	66	170

Table 2. Basic properties of the oxygen-carrier materials.

N2AM1400 was produced by freeze granulation with $MgAl_2O_4$ as support material, and was sintered for 6 hours at 1400ºC. This resulted in spherical particles with comparably high density. Ni18-αAl and Ni21-γAl were produced by dry impregnation of $Ni(NO_3)_2 \times 6H_2O$ onto Al_2O_3, calcination at 550ºC for 30 minutes and sintering at 950ºC for 60 minutes. This procedure resulted in more porous and somewhat less spherical particles than freeze granulation. Ni18-αAl and Ni21-γAl are patent pending.

Due to the higher porosity of Ni21-γAl and Ni18-αAl, a lower bed mass was used compared to N2AM1400. The unfluidized bed heights were between 8.4 and 11.6 cm for fresh particles. For Ni18-αAl, two different bed masses were tested.

3.4 Experimental procedure

Depending on the air and fuel flow, the experiments could be divided into one out of four subcategories:

- CLC - Chemical-looping combustion
  The aim of a CLC experiment was to convert as large share of the fuel as possible to CO_2 and H_2O. This was achieved by using low or modest fuel flow (0.2-0.75 L_n/min) and high air flow (7-10 L_n/min). Natural gas without additional CO_2 and H_2O was used as fuel for all CLC experiments.

- $CLR_{(ng)}$ - Chemical-looping reforming
  The aim of a $CLR_{(ng)}$ experiments was to convert the fuel to CO and H_2. This was achieved by using high fuel flow (0.8-1.5 L_n/min) and moderate to high air flow (3.8-10 L_n/min).

- $CLR_{(H2O)}$ - Chemical-looping reforming with steam
  A chemical-looping reforming experiment where ≈30% steam was added to the natural gas. Adding steam is believed to reduce the formation of solid carbon, and would also increase the production of H_2 via reaction (7). This would mimic conventional auto-thermal reforming, and it seems reasonable to believe that this is the best way to design a chemical-looping reforming process.

- $CLR_{(CO2)}$ - Chemical-looping reforming with CO_2
  A chemical-looping reforming experiment where ≈30% CO_2 was added to the natural gas. Adding CO_2 is believed to reduce the formation of solid carbon, and would also increase the production of CO via reaction (8). This concept has been tested to improve the general understanding of chemical-looping reforming and could be useful for example to produce synthesis gas with high CO/H2 ratio.

Prior to the experiment, the overpressure in the fuel reactor was set to 10-30 Pa by adjusting the level in the water seal. The furnace was heated to a temperature slightly above the desired fuel reactor temperature, which was 800-950°C. During this period both reactor sections were fluidized with air. When sufficiently high temperature was reached, the air to

the fuel reactor was replaced by N_2, and after a minute or two, by fuel. Steady-state conditions were reached after a few minutes, depending on the fuel flow and the oxygen carrier.

Unless else is stated, the data referred to in this paper is from the period following the start-up sequence. Here the process parameters were held constant, and the process was running at as stable conditions as possible. Typically, this period was 1-3 hours. Some experiments with longer running times and variable process parameters have also been conducted.

At the end of each experiment, the oxygen-carrier particles were reoxidized. Most often, the following procedure was used. Fuel and air was replaced with 1 L_n/min N_2 in each reactor part, which resulted in that the solids circulation stopped. After a few minutes, N_2 was replaced with air in both reactor sections. If there was solid carbon present in the fuel reactor, it showed up as CO_2 during the reoxidation. In addition to verifying accumulation of solid carbon, the reoxidation also provided some information about the degree of reduction of the particles in each reactor section, as well as the magnitude of the solids circulation, see section 5.3 below.

4. Evaluation of data

4.1 Composition of the fuel reactor gas

Prior to analysis, the gas from the fuel reactor passed through particle filters, coolers and water traps. Therefore, all measurements were made on dry gas. $x_{CO2,fr}$, $x_{CO,fr}$ and $x_{CH4,fr}$ were measured using infrared analyzers, while $x_{O2,fr}$ was measured with paramagnetic sensors. The gas was also examined with a gas chromatograph, which was necessary to measure $x_{H2,fr}$. In addition to this, it also measured $x_{CO2,fr}$, $x_{CO,fr}$ and $x_{CH4,fr}$. An example of measured concentrations for a $CLR_{(H2O)}$ experiment is shown in Figure 4.

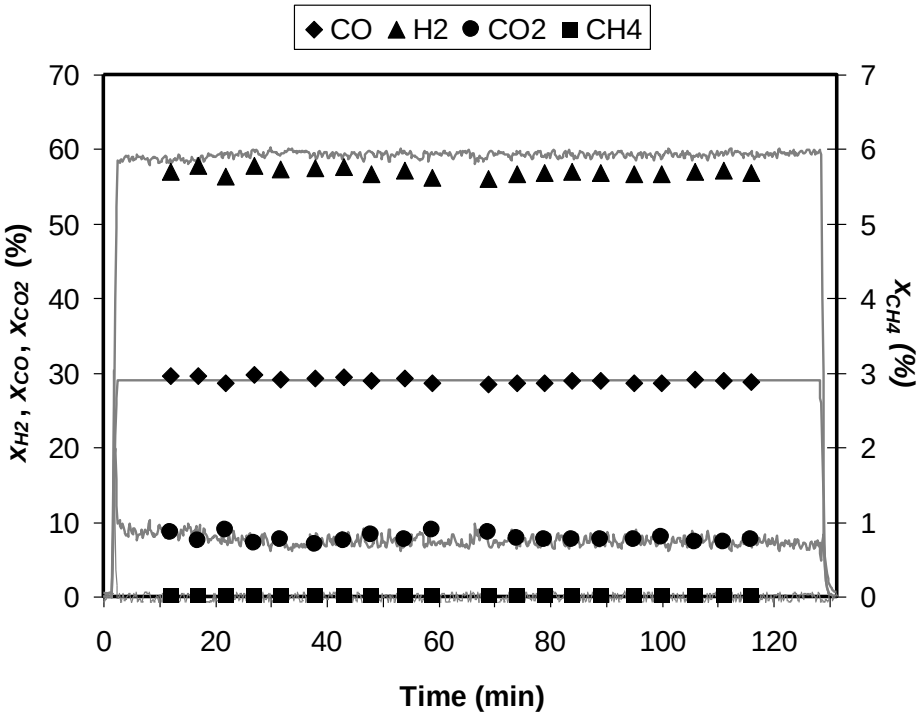

Figure 4. Measured concentrations for 2-hour $CLR_{(H2O)}$ experiment using 250 g N2AM1400 as oxygen carrier with T_{fr}=947ºC, Ψ =37.1% and F_{ng}=1.35 L_n/min. *Ψ is defined in expression (16) below.*

In Figure 4, the dots indicate data points measured with the gas chromatograph and the lines indicate corresponding online data. The $x_{H2,fr}$ line was calculated from the online data under the assumption that there was complete conversion of higher hydrocarbons, that there was no formation of solid carbon in the fuel reactor and that the water-gas shift reaction was at thermodynamical equilibrium. A number $x_{H2O,eq}$ is defined that describes the amount of H_2O that corresponds equilibrium for the dry gas, see expression (10). Since x_i defines the

molar ratio on dry gas, $x_{H2O,eq}$ is a fictionous molar ratio, but it is needed in the calculations below, e.g. to calculate the wet-gas composition. The hydrogen to carbon ratio in the fuel reactor gas, expression (11), will be the same as the hydrogen to carbon ratio for the fuel mix, expression (12). $x_{H2,fr}$ is obtained by combining and solving expressions (10-12). In expression (12), 4.25 represent the amount of H in one unit fuel, while 1.14 is the amount of C.

$$K(T) = \frac{x_{CO2,fr} \times x_{H2,fr}}{x_{CO,fr} \times x_{H2O,eq}} \tag{10}$$

$$(H/C)_{fr} = \frac{x_{H2O,eq} \times 2 + x_{H2,fr} \times 2 + x_{CH4,fr} \times 4}{x_{CO2,fr} + x_{CO,fr} + x_{CH4,fr}} \tag{11}$$

$$(H/C)_{fm} = \frac{\left(1 - y_{H2O,fm} - y_{CO2,fm}\right) \times 4.25 + y_{H2O,fm} \times 2}{\left(1 - y_{H2O,fm} - y_{CO2,fm}\right) \times 1.14 + y_{CO2,fm}} \tag{12}$$

In Figure 4, it can be seen that there was a slight mismatch between $x_{H2,fr}$ obtained by combining expressions (10-12), and $x_{H2,fr}$ measured with the gas chromatograph. With N2AM1400 as oxygen carrier, $x_{H2,fr}$ for CLR experiments measured with the chromatograph was typically 2-3% points below equilibrium. With Ni18-αAl and Ni21-γAl, $x_{H2,fr}$ were closer to equilibrium. Most often, the mismatch was small and should not be of importance for the conclusions of the experiments.

Since N_2 is used as for fluidization gas in the slot and the downcomer, there will be N_2 present in the gas from the fuel reactor. x_{N2} is given by expression (13). The composition of the fuel-reactor gas, including H_2O, can be calculated with expression (14).

$$x_{N2} = 1 - (x_{CO2} + x_{CO} + x_{CH4} + x_{H2} + x_{O2}) \tag{13}$$

$$y_{i,fr} = x_{i,fr} / (x_{CO2,fr} + x_{CO,fr} + x_{CH4,fr} + x_{H2,fr} + x_{O2,fr} + x_{H2O,eq} + x_{N2,fr}) \tag{14}$$

The gas compositions obtained with expressions (10-14) have been the basis for most of the further analysis. An example of the composition of the fuel-reactor gas for a typical $CLR_{(H2O)}$ experiment is shown in Figure 5.

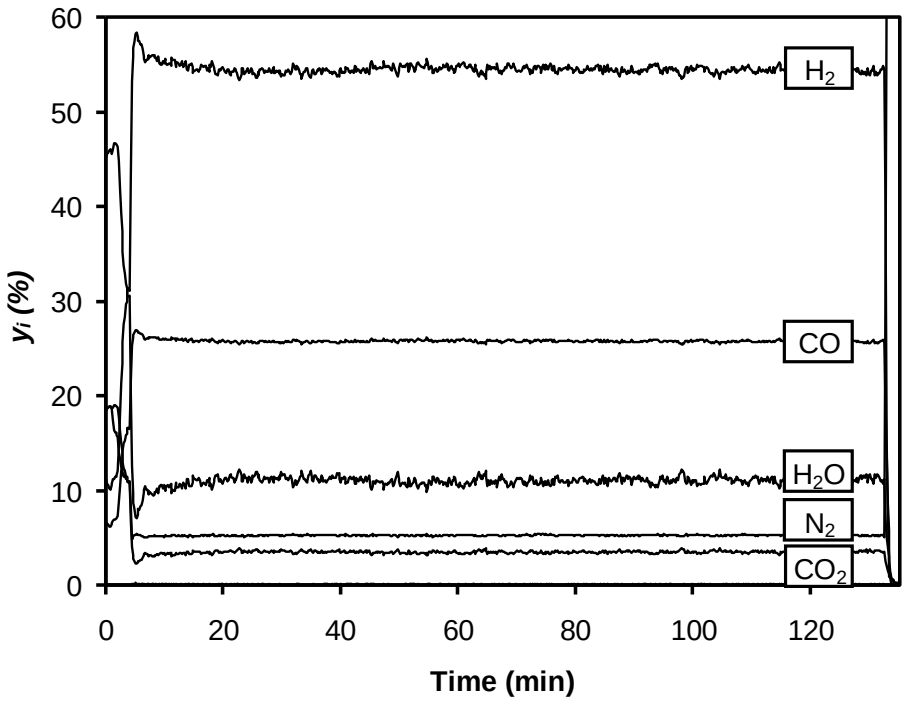

Figure 5. Calculated wet-gas concentration for a 2-hour $CLR_{(H2O)}$ experiment using 170 g Ni21-γAl as oxygen carrier with T_{fr}=951ºC, Ψ =28.8% and F_{ng}=1.36 L_n/min. Ψ is defined in expression 16 below.

4.2 Composition of the air reactor gas

The gas from air reactor passed through particle filters, coolers and water traps prior to analysis, so all measurements were made on dry gas. In this case this is not a problem, since all vital calculations can be done from the dry-gas composition. $x_{CO2,ar}$, $x_{CO,ar}$ and $x_{CH4,ar}$ were measured using infrared analyzers, while $x_{O2,ar}$ was measured with paramagnetic sensors. $x_{H2,ar}$ was set to zero, which should be true since any H_2 that leaks to the air reactor would become oxidized to H_2O more or less instantly. $x_{N2,ar}$ was calculated using expression (13).

The composition of the air-reactor gas was used to make a species balance over the reactor system, as an indicator for carbon formation in the fuel reactor, see section 4.5, to estimate the gas leakage between the reactor sections, see section 4.4, and to calculate the Ψ number, see expression (16).

There was O_2 present in the outlet from the air reactor at most occasions. This was expected for the CLC experiments, but turned out to be the case for CLR experiments using N2AM1400 and Ni21-γAl as well. Since reoxidation of the oxygen-carrier materials, reaction (2), typically is faster than the corresponding reduction reaction. Hence it seems reasonable to

assume that the oxygen carrier particles were more or less completely reoxidized in the air reactor. This shall be compared to some of the CLR experiments when Ni18-αAl was used as oxygen carrier, where there was no O_2 present in the outlet from the air reactor and the oxygen carrier was gradually reduced in both reactor sections until steady-state conditions was achieved. The later behaviour is more in line with earlier chemical-looping reforming experiments by Rydén et al[27,28].

The degree of reduction in each reactor section could be estimated from reoxidation curves, such as the one that is shown in Figure 7 below. The difference in behaviour between the oxygen carriers is likely an effect of differences in reaction kinetics and solids circulation.

4.3 Process performance

The performance of a chemical-looping combustion process can be expressed with the CO_2 yield, γ_{CO2}, which is defined in expression [15].

$$\gamma_{CO2} = x_{CO2,fr} \; / \; (x_{CH4,fr} + x_{CO2,fr} + x_{CO,fr}) \qquad (15)$$

The definition does not take into account the possibility of formation of solid carbon in the fuel reactor, which did occur at some occasions. Neither does it take into account the possibility of higher hydrocarbons being present in the fuel-reactor gas. Higher hydrocarbons are expected to be at least as reactive with NiO as CH_4, and there was rarely any detectable CH_4 in the fuel reactor gas. γ_{CO2} can be said to describe the conversion of natural gas into CO_2 and should be as close to 1 as possible, for a chemical-looping combustion process.

For chemical-looping reforming, the picture is a little more complex. An air factor Ψ can be calculated with expressions (16-19), using the measured oxygen to carbon ratio in the fuel-reactor gas and the known properties of the fuel mix. In expressions (18-19), 0.01 represent the amount of O in one unit fuel, while 1.14 is the amount of C, and 4.41 is the O demand for complete combustion.

$$\Psi = \frac{(O/C)_{fr} - (O/C)_{fm}}{(O/C)_{cc} - (O/C)_{fm}} \qquad (16)$$

$$(O/C)_{fr} = \frac{y_{CO2,fr} \times 2 + y_{H2O,fr} + y_{CO,fr}}{y_{CO2,fr} + y_{CO,fr} + y_{CH4,fr}} \qquad (17)$$

$$(O/C)_{fm} = \frac{\left(1 - y_{H2O,\,fm} - y_{CO2,\,fm}\right) \times 0.01 + y_{H2O,\,fm} + y_{CO2,\,fm} \times 2}{\left(1 - y_{H2O,\,fm} - y_{CO2,\,fm}\right) \times 1.14 + y_{CO2,\,fm}} \quad (18)$$

$$(O/C)_{cc} = \frac{\left(1 - y_{H2O,\,fm} - y_{CO2,\,fm}\right) \times 4.41 + y_{H2O,\,fm} + y_{CO2,\,fm} \times 2}{\left(1 - y_{H2O,\,fm} - y_{CO2,\,fm}\right) \times 1.14 + y_{CO2,\,fm}} \quad (19)$$

A Ψ of 1.0 means that sufficient oxygen has been added to the fuel mix via the solids circulation to burn it into CO_2 and H_2O. A Ψ of 0.26 represents partial oxidation to CO and H_2. It is possible to do experiments with Ψ values below 0.26, since oxygen can also be provided by adding steam or CO_2 to the fuel mix.

In order for Ψ to be useful for evaluating the results of a chemical-looping reforming experiment, there should be very high conversion of natural gas and no or little formation of solid carbon, and the gas composition should be reasonably close to thermodynamic equilibrium. These criteria were fulfilled for the experiments conducted in this study.

The desired value of Ψ for a chemical-looping reforming process depends on factors such as reactor temperature, desired product composition and amounts of H_2O or CO_2 added to the fuel. For a $CLR_{(H2O)}$ process for H_2 production operating at 950ºC and with 30% steam added to the fuel, a Ψ in the order of 0.30-0.35 seems reasonable, see Rydén et al[28,39]. Reducing Ψ further would increase the production of H_2 and CO but result in an endothermic process that would require extensive preheating or external heating.

4.4 Gas leakage between reactor sections

The slot and the downcomer were fluidized with N_2. This resulted in a slight dilution of the gases from the fuel reactor and the air reactor. In addition to this, gas leakage between the reactor sections via the slot and the downcomer is possible.

These phenomena were examined by performing leak tests, during which the loaded reactor was operated at relevant temperatures but without fuel. Instead, air was fed to the air reactor, nitrogen to the slot and the downcomer, and carbon dioxide to the fuel reactor. The gas composition after the reactor sections was measured and it could be calculated how the different gas components distributed themselves within the reactor system. A close examination of the over 200 hours of experimental data have also been done, which provided additional insight into the phenomena.

Most often, the leakage of air to the fuel reactor was zero. On the rare occasions when gas leakage this way could be measured it was very small, typically in the order of ≈0.5% of the total air flow. This means that at least 99%, and in most cases very close to 100%, of the oxygen present in the produced gas should have been transferred there with the solids circulation.

There was always a slight leakage from the fuel reactor to the air reactor. This was likely an effect of the small overpressure applied to the fuel reactor. This leakage typically was in the order of 0.08-0.15 L_n/min. This corresponds to 1.5-4% of the fuel-reactor flow in CLR experiments and 4-20% of the fuel-reactor flow in CLC experiments. The reason for the differing percentages is that CLR uses larger fuel flow compared to CLC.

Between 0.40 and 0.50 L_n/min N_2 was used for fluidization of the downcomer and the slot. Typically, 50-75% of added N_2 ended up in the fuel reactor and the rest in the air reactor. For a CLR experiment, this resulted in a N_2 concentration in the outlet from the fuel reactor of 3-13%. For CLC experiments, the N_2 concentration was 11-35%. The reason why the dilution becomes higher for CLC experiments is that the fuel flow is smaller in these experiments compared to CLR, while the same amounts of fluidization gas still are needed for the slot and the downcomer. 70-80% of the N_2 was added to the downcomer, which has an exit that is located above the particle bed, which is where the chemical reactions should take place. Hence it seems unlikely that the N_2 dilution would have had any significant impact on the experimental results.

4.5 Carbon formation

One of the crucial criteria for oxygen-carrier materials is that they should not promote formation of solid carbon in the fuel reactor. This could happen since it is well known that metallic Ni catalyses reactions (4-5). Due to the nature of the reactor system used, it was not possible to make exact calculations of the carbon formation. It was possible to make estimations though.

Firstly, since the composition of the fuel mix is known and all major components excluding H_2O are measured, the carbon formation can be calculated from the species balance, if it is assumed that the gas mixture is at thermodynamical equilibrium for the water-gas shift reaction. However, as is pointed out in Figure 4 and section 4.1 above, measured values of H_2 were occasionally slightly lower than the corresponding equilibrium values, which would indicate negative carbon formation under these assumptions. Therefore, it is

doubtable that this method provides an accurate picture, especially if only minor carbon formation occurs.

Secondly, it is possible to estimate carbon formation by measuring the CO_2 concentration in the outlet from the air reactor. The assumption that needs to be made for this method to be valid is that if there is carbon formation, most of the carbon will follow the particle circulation to the air reactor and burn there. The fraction of added carbon that ends up in the air reactor can be calculated with expression (20).

$$C_{ar} / C_{tot} = \frac{F_{ar,dry,out} \times x_{CO2,ar}}{F_{ng,fr} \times 1.14 + F_{CO2,fr}} \tag{20}$$

In expression (20), the numerator represents the amount of carbon that ends up in the air reactor, while the denominator represents the amount of carbon added to the fuel reactor. The problem with this method is that the gas leakage from the fuel reactor to the air reactor contains CO, CO_2 and possibly CH_4 that has to be taken into consideration. As mentioned in section 4.4 above, this leakage typically was 0.08-0.15 L_n/min, which corresponds to 1.5-4% of the fuel reactor flow in $CLR_{(H2O)}$ experiments. Hence it can be assumed that C_{ar}/C_{tot} value of 1.5-4% indicates that there is no or very little formation of solid carbon in the fuel reactor, while C_{ar}/C_{tot} values above 4% indicate that there is. If the leakage is set to $F_{fr \rightarrow ar}$, the carbon formation in absolute numbers can be estimated with expression (21).

$$C_{ar} / C_{tot} = \frac{F_{ar,dry,out} \times x_{CO2,ar} - F_{fr \rightarrow ar} \times \left(y_{CO2,fr} + y_{CO,fr} + y_{CH4,fr} \right)}{F_{ng,fr} \times 1.14 + F_{CO2,fr}} \tag{21}$$

In expression (21), the numerator represents the amount of CO_2 from the air reactor that is estimated to be due to solid carbon from the fuel reactor. $F_{fr \rightarrow ar}$ is believed to have been in the order of 0.1 L_n/min for most experiments. For $CLR_{(H2O)}$ experiments, this means that C/C_{tot} calculated with expression (21) would be ≈2% lower than C_{ar}/C_{tot}. Choosing a higher number for $F_{fr \rightarrow ar}$ would result in lower C/C_{tot} values, and vice versa. The general principles behind expressions (20-21) are illustrated in Figure 6.

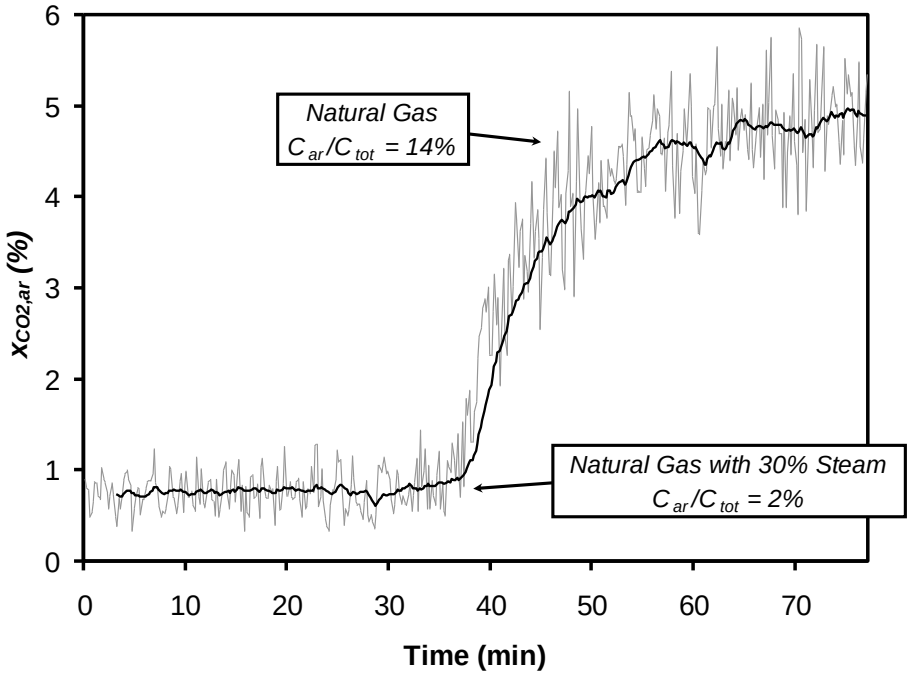

Figure 6. $x_{CO2,ar}$ as function of time for a $CLR_{(H2O)}$ experiment using 170 g Ni21-γAl as oxygen carrier, where the steam saturation of the fuel is turned off after 35 minutes.

In Figure 6, it can be seen that turning steam saturation off increases the carbon leakage to the air reactor greatly. C_{ar}/C_{tot} calculated via expression (20) increases from 2% to 14%. C/C_{tot} calculated via expression (21) with $F_{fr\rightarrow ar}$ set to 0.1 L_n/min becomes 14-2=12%. If the gas leakage between the reactor sections is constant this implies that the 12% points increase in carbon transferred to the air reactor is due to solid carbon transferred to the air reactor via the particle circulation.

The problem with expressions (20-21) is that the real value of $F_{fr\rightarrow ar}$ is rather uncertain. Hence C_{ar}/C_{tot} and C/C_{tot} calculated with expressions (20-21) shall be seen only as an indication of the level of carbon formation, not as absolute numbers. Nonetheless, for N2AM1400 or Ni21-γAl the obtained numbers whit $F_{fr\rightarrow ar}$ set to 0.1 L_n/min were predictable and corresponded reasonably well with other indicators. This was not the case for Ni18-αAl, where the CO_2 content in the air reactor gas varied greatly between different experiments, a phenomenon that is discussed in section 5.2 below.

The final method to determine if there was carbon formation during a particular experiment is to see if there is any carbon accumulation within the reactor system. During the course of the experiments, carbon was found to get stuck at various locations connected to the fuel reactor, such as the pressure measuring taps and possibly also in the particle separation

box. Minor amounts could also be present directly in the fuel reactor. During reoxidation, accumulated carbon is burnt to CO_2, see Figure 7.

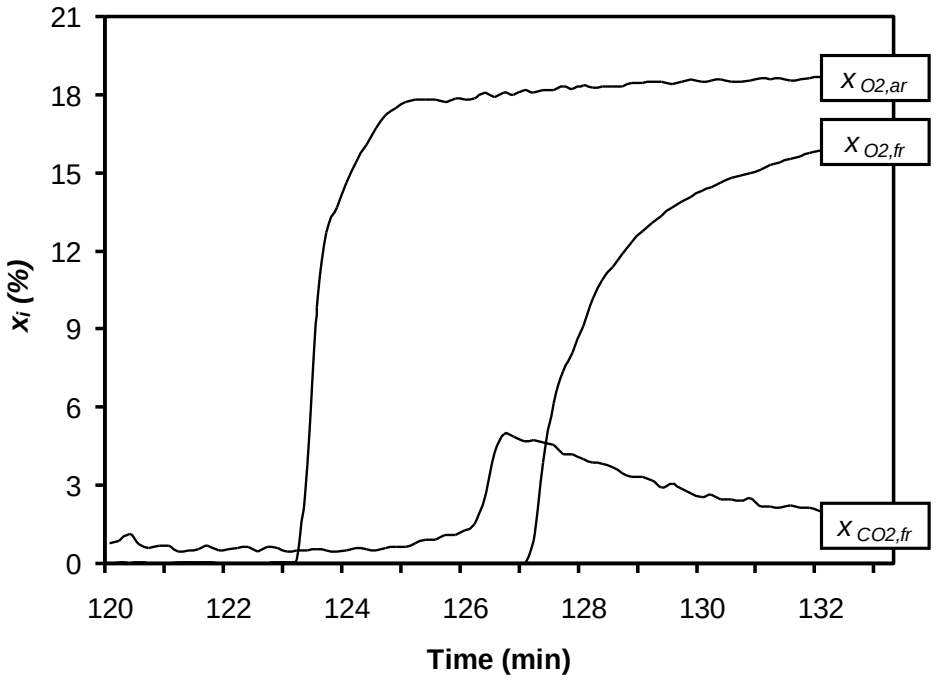

Figure 7. Reoxidation following a 2-hour $CLR_{(CO2)}$ experiment with N2AM1400 as oxygen carrier, air is introduced after ≈123 min, the carbon accumulation corresponds to ≈0.1% of added carbon.

In Figure 7, both reactors are fluidized with N_2 prior to reoxidation. In the air reactor, the oxygen carrier is almost completely oxidized, hence the O_2 concentration responds rapidly once the N_2 is switched to 2 L_n/min air. In the fuel reactor, N_2 is switched to1 L_n/min air. Here added O_2 is initially consumed by the reoxidation of the reduced oxygen carrier. After a few minutes some CO_2 is produced. The solid carbon lasts several minutes after the breakthrough of O_2 in the fuel reactor, which indicates that much of it is accumulated where its opportunity to react with air is limited, such as the pressure measuring taps. The reason why x_{O2} in Figure 7 does not reach 21% is dilution with N_2 that is used for fluidization of the slot and downcomer.

The amount of accumulated carbon can be expressed as the percentage of the total amount of carbon added to the reactor, see expression (22).

$$C_{ack}/C_{tot} = (CO_2 \text{ released during reoxidation}) / (\text{Total carbon added to the fuel reactor}) \qquad (22)$$

The amount of carbon released during reoxidation can be estimated by integrating the obtained CO_2 curve, i.e. it corresponds to the area under the CO_2 curve in Figure 7.

Carbon accumulation should be a reliable indicator for whether or not there was formation of solid carbon in the fuel reactor during the experiments, but it does probably not give a good picture of the magnitude. For $CLR_{(H2O)}$ and $CLR_{(CO2)}$ experiments, the amount of accumulated carbon was never above 0.24% of the total amount of carbon added to the system during the whole experiment. In most cases the CO_2 peak during reoxidation was barely detectable. For CLC experiments with Ni21-γAl and Ni18-αAl, where natural gas without H_2O or CO_2 was used, the carbon accumulation was more substantial and estimated to 0.4-2.0%. For $CLR_{(ng)}$ experiments with these oxygen carriers the carbon accumulation was even larger. It seems reasonably safe to conclude that adding 30% H_2O or CO_2 to the fuel reduced carbon formation significantly, as is illustrated by Figure 6.

5. Results

In total, over 160 hours of continuously operating experiments with fuel have been recorded, distributed among the experiment types and oxygen carriers as is shown in Table 3.

	CLC (h)	$CLR_{(ng)}$ (h)	$CLR_{(H2O)}$ (h)	$CLR_{(CO2)}$ (h)	Total h)
N2AM1400	10	7	35	7	59
Ni18-αAl	21	4*	27	5	57
Ni21-γAl	5	11*	24	2	42
Total (h)	36	22	86	14	158

*Table 3. Hours of operation with fuel for each type of experiment and oxygen carrier, * indicate that there were problems running this type of experiments due to large formation of solid carbon in the fuel reactor.*

Not included in Table 3 are experiments that lasted for less than 30 minutes. These short experiments amount to perhaps 10 hours totally. The total time each oxygen carrier has been fluidized at hot conditions is roughly 50% greater than the total time with fuel.

5.1 Chemical-looping combustion

Natural gas was used as fuel for all chemical-looping combustion experiments. No CH_4 was detected in the outlet from the fuel reactor, so the conversion of natural gas was very close to 100%. Unfortunately, the selectivity towards CO_2 was not equally good. Here it shall be pointed out that the examined oxygen-carrier materials were chosen for testing because they had shown promise for chemical-looping reforming applications in early screenings using batch-fluidized bed reactors, so this was not that surprising. For a chemical-looping reforming, high conversion of CH_4 into CO and H_2 is ideal.

Key data for CLC experiments with stable process parameters can be found in Table 4. It shall be pointed out that many of the CLC experiments were made with varying process parameters, and are therefore not included in the table since the data varied greatly during operation.

Oxygen Carrier	*Duration (min)*	T_{fr} (ºC)	F_{ng} (L_n/min)	$y_{CO2,fr}$ (%)	$y_{CO,fr}$ (%)	$y_{CH4,fr}$ (%)	$y_{H2,fr}$ (%)	$y_{H2O,fr}$ (%)	$y_{N2,fr}$ (%)	Ψ (%)	γ_{CO2} (%)	C/C_{tot}* (%)	C_{ack}/C_{tot} (%)
N2AM1400	128	946	0.25	22.3	2.2	0	2.8	42.8	29.9	94.7	91.2	0.2	0
N2AM1400	128	948	0.49	24.1	4.3	0	5.7	47.2	18.7	90.8	84.8	0.9	0
N2AM1400	125	948	0.72	22.2	8.1	0	11.1	45.3	13.4	83.6	73.3	0.3	0
N2AM1400	46	952	0.49	25.0	3.7	0	4.8	48.6	18.0	92.4	87.2	1.4	0
Ni21-γAl	81	941	0.48	12.0	18.6	0	30.0	28.1	11.3	59.2	39.2	2.3	2.01
Ni21-γAl	107	870	0.48	15.1	13.1	0	22.6	30.9	18.2	67.4	53.5	7.7	1.67
N18-αAl	61	950	0.49	25.4	1.9	0	2.4	48.5	21.8	95.9	93.1	5.1	0.44
N18-αAl	58	948	0.41	25.3	2.7	0	3.5	48.7	19.7	94.3	90.4	2.7	1.05
N18-αAl	30	954	0.40	25.5	2.8	0	3.6	49.2	18.9	94.2	90.2	2.8	no data
N18-αAl	63	949	0.50	22.9	0.7	0	1.0	43.2	32.2	98.2	96.9	13.8	0.80
N18-αAl	80	900	0.49	22.3	2.1	0	3.0	42.3	30.3	94.6	91.5	13.6	1.01
N18-αAl	65	848	0.49	22.3	2.5	0	4.3	42.0	28.9	92.9	89.8	14.1	0.63
N18-αAl	65	952	0.49	22.3	2.8	0	3.5	43.1	28.4	93.5	89.0	12.5	no data
N18-αAl	125	951	0.49	24.3	1.3	0	1.7	47.0	25.7	96.9	94.8	5.3	1.86
N18-αAl	120	950	0.72	25.3	4.1	0	5.4	49.4	15.8	91.7	86.1	3.4	no data
N18-αAl	110	945	0.24	21.6	0.7	0	0.9	40.8	36.0	98.1	96.7	9.9	1.90
N18-αAl	55	964	0.49	25.0	0.6	0	0.9	56.4	17.1	98.5	97.6	5.9	no data

*Table 4. Data for CLC experiments with stable process parameters. The numbers are average values for the whole experiment. * C/C_{tot} calculated with $F_{fr\rightarrow ar}$ set to 0.1 L_n/min.*

Two factors were found to be of importance to achieve high γ_{CO2}, namely fuel reactor temperature and oxygen-carrier loading, see Figures (8-9).

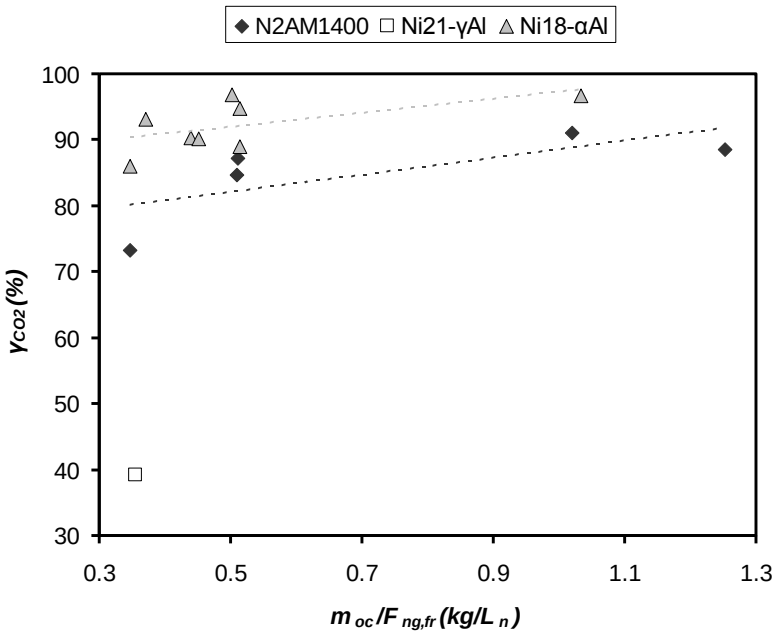

Figure 8. γ_{CO2} as function of the fuel to oxygen-carrier ratio. Each dot represents average values for 1-2 hours of experiments with stable process parameters and $T_{fr}\approx$950ºC, or represents periods of steady-state operation from experiments with varying fuel flow. m_{oc} is the mass of oxygen carrier added to the reactor.

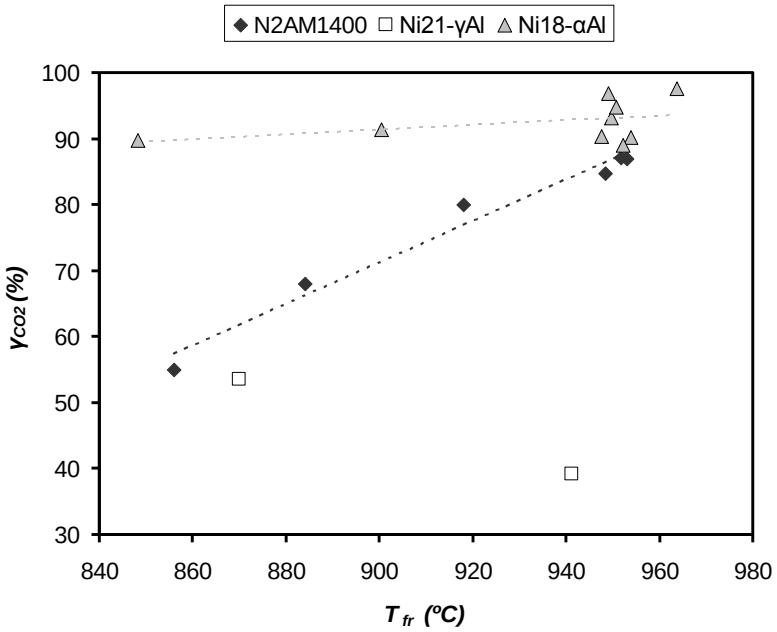

Figure 9. γ_{CO2} as function of the fuel reactor temperature. Each dot represents average values for 1-2 hours of experiments with stable process parameters and F_{ng}≈0.5 L_n/min, or represents periods of steady-state operation from experiments with varying temperature.

The air to fuel ratio may also have had some influence on the results. For Ni18-αAl, four hours of experiment were made where the air flow was changed stepwise between 5 L_n/min and 9 L_n/min, while the fuel flow was held constant at 0.53 L_n/min. Here γ_{CO2} increased from about 86% to 88%. This could have been due to increased solids circulation and increased availability of oxygen in the fuel reactor, but the interpretation is uncertain because Ni18-αAl provided somewhat unstable results, as can be seen in Figures (8-9). The effect of changes in the fuel to air ratio was not examined closely for N2AM1400 or Ni21-γAl.

Ni18-αAl was used for 21 hours of CLC experiments. In Figures (8-9), it can be seen that this was the oxygen carrier that provided the highest CO_2 yield. Unfortunately, it also showed some unexpected drawbacks. Firstly, there was formation of solid carbon in the fuel reactor. C_{ack}/C_{tot} was 0.4-1.9%. C/C_{tot} calculated via expression (21) was 3-14%, but as will be explained further in section 5.2 below, the carbon leakage to the air reactor seems to have varied greatly when Ni18-αAl was used as oxygen carrier. Hence the actual numbers for the carbon formation may not necessarily have been that high. Secondly, Ni18-αAl changed reactivity during and in between different experiments. Fresh particles provided remarkably high selectivity towards CO_2. For the initial 20 minutes of CLC experiments using fresh particles, γ_{CO2} was over 99% with 0.45 L_n/min fuel at 900ºC. The results declined rapidly

though, until some kind of steady-state was reached after a few hours. The particles could be partially regenerated by running a $CLR_{(H2O)}$ experiment with high H_2 concentration, only to loose reactivity again after an hour or so of CLC experiments. The reason for this behaviour is not known, but the mentioned deactivation and regeneration behaviour have been demonstrated in lab scale as well, using a batch fluidized-bed reactor. The numbers presented in Table 4 and Figures (8-9) are for steady-state operations, when the results were far from as good as for fresh particles. Still, it can be seen γ_{CO2} varies quite much between experiments using otherwise similar process parameters.

N2AM1400 was used for 10 hours of CLC experiments. N2AM1400 provided predictable and stable results. The carbon leakage to the air reactor was small and no carbon accumulation was detected, so there was most likely no formation of solid carbon in the fuel reactor. γ_{CO2} was low compared to Ni18-αAl, and the results were very sensitive to fuel reactor temperature, as can be seen in Figure 9.

Ni21-γAl was used for 5 hours of CLC experiments. This oxygen carrier provided very low γ_{CO2} and there was also carbon formation, approximately at the same extent as for Ni18-αAl. This oxygen carrier is not suitable for chemical-looping combustion applications.

To put the chemical-looping combustion results into some perspective, it is worth citing the work of Johansson et al[9,19], who examined chemical-looping combustion of natural gas using a similar experimental setup as the one used here. With 340 g freeze granulated oxygen-carrier particles consisting of 60% NiO supported on $MgAl_2O_4$, the resulting γ_{CO2} was above 98.5% for most fuel flows and reactor temperatures that was examined. No formation of solid carbon in the fuel reactor was reported. This could possibly be because the methodology and reactor setup used in these experiments made it hard to detect carbon formation.

5.2 Chemical-looping reforming

In general, the results for the chemical-looping reforming experiments were highly encouraging. The experiments ran smoothly and with some steam or CO_2 added to the fuel it was possible to operate the reactor at very low Ψ values with no carbon accumulation, and seemingly very little carbon formation. It was even possible to use Ψ values below the stoichiometric ratio for partial oxidation by supplying excess oxygen with H_2O or CO_2. The conversion of natural gas into reagents was very high for all three materials. For low Ψ values and temperatures, minor amounts of CH_4 could be expected due to thermodynamical constraints.

Key data for $CLR_{(H2O)}$, $CLR_{(CO2)}$ and $CLR_{(ng)}$ experiments with stable process parameters can be found in Tables (5-7). It shall be noted that for most of $CLR_{(ng)}$ experiments, there was so much carbon formation (C/C_{tot}>20%) that the numbers becomes highly uncertain. Hence these experiments have not been included. Neither have experiments where the process parameters were altered during operation.

Oxygen Carrier	*Duration (min)*	T_{fr} (ºC)	F_{ng} (L_n/min)	$y_{CO2,fr}$ (%)	$y_{CO,fr}$ (%)	$y_{CH4,fr}$ (%)	$y_{H2,fr}$ (%)	$y_{H2O,fr}$ (%)	$y_{N2,fr}$ (%)	Ψ (%)	C/C_{tot}* (%)	C_{ack}/C_{tot} (%)
N2AM1400	129	947	0.85	13.4	14.7	0	26.8	36.2	8.8	61.7	-0.4	0
N2AM1400	128	947	1.33	7.7	21.9	0	43.5	22.7	4.2	42.6	0	0.04
N2AM1400	123	947	1.35	6.1	23.9	0	48.8	18.4	2.8	37.1	-0.1	0
N2AM1400	137	946	1.30	4.8	25.1	0.01	52.2	14.7	3.2	32.8	-0.3	0
N2AM1400	122	948	1.29	3.7	25.3	0.02	53.4	11.5	6.1	29.5	-0.3	0
N2AM1400	130	950	1.29	4.8	24.6	0	51.0	14.8	4.9	33.2	-0.2	0
N2AM1400	120	870	1.36	6.3	22.5	0.03	48.5	16.0	6.7	35.9	2.7	0.01
N2AM1400	120	870	1.33	5.5	23.0	0.04	49.8	14.2	7.4	33.8	2.3	0
N2AM1400	133	800	1.31	6.1	22.5	0.42	50.9	13.3	6.8	32.9	7.1	0.01
N2AM1400	132	799	1.29	4.1	24.4	0.60	55.2	8.9	6.8	27.0	5.0	0.11
N2AM1400	122	800	1.22	2.7	25.2	0.95	56.8	6.0	8.3	22.9	5.3	0.09
N2AM1400	238	948	1.20	2.7	27.4	0.02	58.8	8.5	2.6	25.6	-0.1	0
N2AM1400	234	949	1.16	1.8	27.7	0.18	60.2	5.9	4.1	22.5	0	0.24
N2AM1400	209	949	1.35	4.7	25.5	0	53.0	14.6	2.3	32.5	-0.1	0
Ni21-γAl	80	865	1.50	5.0	23.4	0.05	50.9	12.7	7.9	32.0	10.3	0
Ni21-γAl	78	869	0.95	5.9	22.7	0.01	48.9	15.1	7.5	34.9	2.6	0
Ni21-γAl	72	879	0.95	8.0	19.8	0	41.8	20.5	9.9	42.5	8.4	0.03
Ni21-γAl	118	871	1.39	2.6	26.4	0.14	58.0	7.0	5.9	24.3	0.7	0.01
Ni21-γAl	100	798	0.90	6.2	21.1	0.19	47.9	13.2	11.4	34.0	11.5	0.10
Ni21-γAl	108	800	1.33	3.9	24.2	0.51	54.6	8.5	8.3	26.7	9.6	0.07
Ni21-γAl	120	951	0.95	8.8	19.1	0.01	37.1	25.6	9.4	47.8	1.9	0
Ni21-γAl	114	950	1.36	4.4	24.3	0.03	50.7	13.6	7.0	32.2	0.8	0
Ni21-γAl	248	948	1.19	2.0	27.5	0.08	59.5	6.5	4.4	23.3	-0.2	no data
Ni21-γAl	200	940	1.13	0.8	28.5	0.88	63.2	2.8	3.9	18.2	-0.1	no data
Ni21-γAl	73	938	1.12	0.6	28.7	1.32	63.6	2.3	3.5	17.3	0.2	no data
Ni21-γAl	140	951	1.36	3.5	25.7	0.02	54.4	11.1	5.3	28.8	0.2	0.04
N18-αAl	127	951	0.85	13.0	14.0	0	25.2	35.0	12.9	62.3	5.4*	0
N18-αAl	127	944	1.22	7.1	20.8	0	41.7	21.0	9.4	42.1	4.0*	0
N18-αAl	158	948	1.43	8.8	19.6	0	38.2	25.5	8.0	47.3	6.0*	0
N18-αAl	102	937	1.34	4.5	23.2	0.02	48.4	13.5	10.4	32.8	0.2*	no data
N18-αAl	75	935	1.33	3.4	23.9	0.06	50.9	10.2	11.6	28.8	0*	0
N18-αAl	110	950	1.37	5.3	23.6	0	48.6	16.2	6.3	35.2	6.2*	0
N18-αAl	110	870	1.43	7.6	21.2	0	45.2	19.4	6.6	40.2	4.0*	0
N18-αAl	80	870	1.40	5.5	23.0	0	49.7	14.2	7.6	33.9	3.7*	0
N18-αAl	122	870	1.38	3.8	25.0	0.03	54.5	10.0	6.6	28.3	1.4*	0
N18-αAl	97	800	1.43	7.0	21.8	0.10	49.5	15.0	6.6	35.6	5.7*	0
N18-αAl	88	800	1.36	4.2	24.4	0.26	55.2	9.0	6.9	27.5	1.6*	0
N18-αAl	148	950	1.39	3.7	25.3	0.01	53.3	11.6	6.1	29.6	0*	0
N18-αAl	120	935	1.39	2.6	26.7	0.02	57.5	8.1	5.2	25.3	-0.5*	0

*Table 5. Some key data for $CLR_{(H2O)}$ experiments with stable process parameters. The numbers are average values for the whole duration of the experiment. * C/C_{tot} calculated with $F_{fr\rightarrow ar}$ set to 0.1 L_n/min, possibly not valid for N18-αAl.*

Oxygen Carrier	*Duration (min)*	T_{fr} (ºC)	F_{ng} (L_n/min)	$y_{CO2,fr}$ (%)	$y_{CO,fr}$ (%)	$y_{CH4,fr}$ (%)	$y_{H2,fr}$ (%)	$y_{H2O,fr}$ (%)	$y_{N2,fr}$ (%)	Ψ (%)	C/C_{tot}* (%)	C_{ack}/C_{tot} (%)
N2AM1400	120	950	1.47	6.3	34.2	0	42.7	11.7	5.1	31.5	0.2	0.04
N2AM1400	114	946	1.43	5.3	37.5	0	44.7	9.4	3.1	26.5	-0.1	no data
N2AM1400	113	942	1.43	2.4	38.4	0.04	49.8	4.6	4.7	21.5	-0.2	0.10
N2AM1400	60	869	1.47	4.9	35.2	0.04	46.3	7.6	6.0	26.7	5.1	0.09
Ni21-γAl	96	951	1.49	3.5	37.5	0.01	48.5	6.8	3.7	24.7	0.5	0
N18-αAl	85	933	1.49	3.0	35.7	0.04	46.6	5.6	9.1	23.7	-0.1*	0.09
N18-αAl	105	843	1.48	6.0	32.2	0.04	42.8	8.7	10.2	29.4	6.2*	0.06
N18-αAl	115	950	1.49	6.6	32.3	0.01	40.2	12.2	8.8	33.1	3.3*	0.02

*Table 6. Some key data for $CLR_{(CO2)}$ experiments with stable process parameters. The numbers are average values for the whole duration of the experiment. * C/C_{tot} calculated with $F_{fr\rightarrow ar}$ set to 0.1 L_n/min, possibly not valid for N18-αAl.*

Oxygen Carrier	*Duration (min)*	T_{fr} (ºC)	F_{ng} (L_n/min)	$y_{CO2,fr}$ (%)	$y_{CO,fr}$ (%)	$y_{CH4,fr}$ (%)	$y_{H2,fr}$ (%)	$y_{H2O,fr}$ (%)	$y_{N2,fr}$ (%)	Ψ (%)	C/C_{tot}* (%)	C_{ack}/C_{tot} (%)
N2AM1400	133	950	1.22	14.7	17.8	0	27.1	33.4	7.1	64.1	1.7	no data
N2AM1400	135	948	1.44	10.2	21.8	0	35.2	24.4	8.4	53.7	2.3	0.06
N2AM1400	130	950	1.43	6.8	25.9	0	43.9	17.0	6.3	44.5	1.6	0.04

*Table 7. Some key data for $CLR_{(ng)}$ experiments with stable process parameters. The numbers are average values for the whole duration of the experiment. * C/C_{tot} calculated with $F_{fr\rightarrow ar}$* set to 0.1 L_n/min.

In most cases, the fuel reactor gas appears to have been close to thermodynamic equilibrium. For N2AM1400 and Ni21-γAl the CH_4 concentration was slightly above equilibrium, but the numbers were still quite small. As mentioned in section 4.1 above, the H_2 concentrations was slightly below equilibrium for N2AM1400.

In Figure 10, data for CLR experiments with stable process parameters using N2AM1400 and Ni21-γAl as oxygen carrier have been put into a C/C_{tot}-T_{FR}-diagram. Each dot represents the average data for a single experiment lasting 1-4 hours each. C/C_{tot} is calculated using expression (21), with $F_{fr\rightarrow ar}$ set to 0.1 L_n/min.

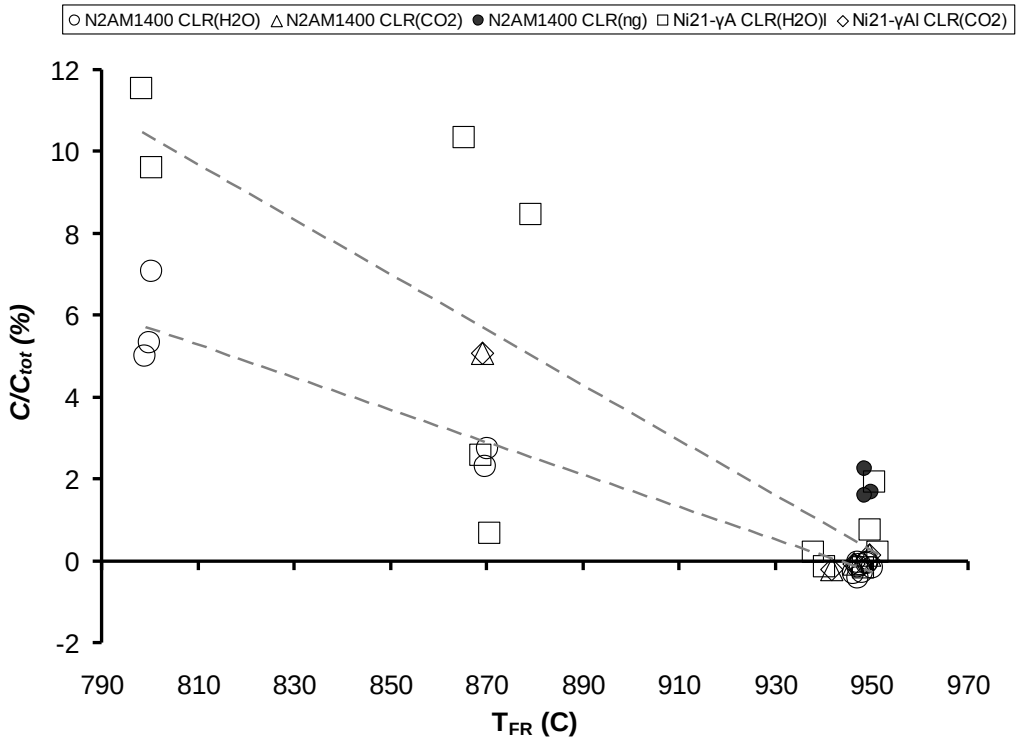

Figure 10. C/C_{tot} as function of fuel-reactor temperature for CLR experiments, when N2AM1400 and Ni21-γAl are used as oxygen carrier.

In Figure 10, it can be seen that the carbon leakage to the air reactor increased as the fuel-reactor temperature was reduced. This corresponds decently with the cases with distinct carbon accumulation. At temperatures above 930ºC estimated C/C_{tot} was 0 for almost all cases. No correlation between C/C_{tot} and Ψ could be established.

For N2AM1400, all results were consistent and predictable. The rare instances when any carbon accumulation was detected, it was below 0.2% of the total amount of carbon added to the system.

For Ni21-γAl, there were two $CLR_{(H2O)}$ experiments at 870ºC where expressions (20-21) indicated that there should be substantial carbon formation, but where no carbon accumulation took place in the reactor. These were the first two experiments with this particular oxygen carrier. The reason why the results differed so much from the other experiments with thus oxygen carrier is not clear. It may have to do with the fact that Ni21-γAl experienced considerable change in density during operation, as is explained in section 5.4 below. This would give a decrease of the level of particles in the reactor sections, and may have had an effect on the gas leakage between the reactors. With the exception of these two occasions, the numbers were about the same as for N2AM1400.

For Ni18-αAl, the picture was a little more confusing. As can be seen in Tables (5-6), it can be seen that the Ψ values achieved was as good as for the other oxygen carriers, and that there was no accumulation of carbon in the reactor for any of the $CLR_{(H2O)}$ experiments where the fuel reactor temperature was 870ºC or above. However, the carbon leakage to the air reactor calculated with expressions (20-21) varied greatly. The most likely explanation for this is that the gas leakage from the fuel reactor to the air reactor was larger and varied more for Ni18-αAl compared to the other two oxygen carriers. This may have had to do with factors such as too high particle levels in the reactors, too low overpressure in the fuel reactor, or too low flow of fluidization gas to the downcomer.

Chemical-looping reforming with only natural gas as fuel resulted in substantial carbon formation for Ni21-γAl and Ni18-αAl. C/C_{tot} estimated with expressions (20-21) was from 15% and upwards, which is illustrated in Figure 6. For N2AM1400 the carbon formation was less severe, and estimated to ≈2% with $\Psi=44.5\%$ at 950ºC, using expressions (20-21).

5.3 Degree of reduction and solids circulation

The degree of reduction of the oxygen carrier can be estimated from reoxidation curves, such as the one shown in Figure 7, where the air flow and response time gives amount of O_2 required for reoxidation. The difference in the degree of reduction between the air reactor and the fuel reactor gives the magnitude of the solids flow from the air reactor to the fuel reactor, as well as the residence time of the oxygen carrier. It shall be pointed out that the accuracy of these estimations is low because of a considerable delay period in the gas feeding system, the possibility of mixing of bed material via the slot in the bottom of the reactor and the lack of precise knowledge about the amount of particles in each reactor section.

In the air reactor, the particles were close to completely oxidized for most of the experiments, with the exception of CLR experiment with Ni18-αAl as oxygen carrier. For CLC experiments, less than 15% of the oxygen was removed in the fuel reactor. For CLR experiments, it is estimated that 20-45% of the oxygen was removed in the fuel reactor when N2AM1400 was used as oxygen carrier. The corresponding numbers for Ni21-γAl was 15-20%. For the experiments with Ni18-αAl where there was no O_2 in the outlet from the air reactor, the degree of reduction was 30-45% in the air reactor and 70-80% in the fuel reactor. The solids circulation between the reactor sections was estimated to 1.0-2.5 g/s for N2AM1400 and Ni18-αAl, and 2.0-3.5 g/s for Ni21-γAl. This corresponds to a residence time in the fuel reactor in the order of to 60-120 seconds for N2AM1400 and Ni18-αAl, and 30-60 seconds for Ni21-γAl.

These numbers indicate that the high selectivity towards H_2 and CO during CLR experiments was due to of lack of oxygen available on the oxygen-carrier particles, except possibly for the experiments with Ni18-αAl. Slow reaction rate between the oxygen carrier and CO/H_2 seems like a more probable explanation.

5.4 Effects on the oxygen-carrier particles

Of the tested oxygen-carrier materials, N2AM1400 was the one that provided most consistent results. It was used for 35 hours of $CLR_{(H2O)}$, 7 hours of $CLR_{(CO2)}$, 7 hours of $CLR_{(ng)}$ and 10 hours of CLC experiments. There were no problems with agglomerations or defluidization. N2AM1400 seems to have been stable. The used particles were examined with microscope, scanning electron microscope and by x-ray diffraction. No changes in the surface or the phase composition could be detected, compared to fresh particles. The density, porosity and size distribution of the particles did not change in any measurable way.

Ni18-αAl was used for 27 hours of $CLR_{(H2O)}$, 5 hours of $CLR_{(CO2)}$ and 21 hours of CLC experiments. In addition to this, 4 hours of problematic experiments with very high carbon formation (C/C_{tot}>10%) were recorded. These were attempts to do $CLR_{(ng)}$ experiments, which did not turn out well. Ni18-αAl seems to have been stable. The used particles looked slightly less porous than the fresh, both in the scanning electron microscope and in conventional microscope. The apparent density of the particles had increased by 9%. They still looked intact though. According to the x-ray diffraction analysis, no new phases occurred in the used particles.

Ni21-γAl was used for 24 hours of $CLR_{(H2O)}$, 5 hours of $CLR_{(CO2)}$ and 2 hours of CLC experiments. In addition to this, 11 hours of problematic experiments with very high carbon formation (C/C_{tot}>10%) were recorded. These were attempts to do $CLR_{(ng)}$ experiments that did not turn out well. Ni21-γAl changed considerably during operation. The fresh particles were comparably large and porous, while the used ones were less so. The apparent density had increased 40%. The used Ni21-γAl particles were still highly reactive, so whatever happened to them did not deactivate them. It was not possible to verify any changes on the particles with x-ray diffraction analysis. It can not be ruled out that the large change in particle density may have had some impact on the experiments, since this must have resulted in gradually decreased bed height in the reactor sections, and that an increasing fraction of the particles became bound to the downcomer. Notably, considerable amounts of CH_4 were detected for some of the $CLR_{(H2O)}$ experiments.

6. Discussion

The experiments presented in this paper show that chemical-looping reforming should be feasible. Complete conversion of natural gas and very high selectivity towards the desired products was achieved with all tested oxygen-carrier materials. There were no problems with defluidization or agglomerations, despite the sometimes quite harsh experimental conditions.

As has been mentioned numerous times, there was formation of solid carbon in the fuel reactor at some occasions, especially when natural gas without H_2O or CO_2 was used as fuel and when the fuel reactor temperature was low. This is not necessarily a big problem. If the carbon follows the oxygen-carrier particles to the air reactor it would burn there and release heat that could be used for the endothermic reformer reactions in the fuel reactor. This would dilute the N_2 from the air reactor with CO_2 though, so if the chemical-looping process is to be utilized for production of heat, power or H_2 with CO_2 capture, carbon formation in the fuel reactor would lead to reduced capture efficiency.

It shall be noted that reforming of hydrocarbons results in a very large volumetric increase, see reactions (6-8). Therefore, the power required for compression of produced H_2 or synthesis gas to suitable product pressure becomes considerable for any process working at atmospheric pressure. As a consequence, elevated pressure during the reforming process would be highly beneficial for the overall efficiency, see Rydén et al[27,39]. If the process is pressurized, the thermodynamics indicate that higher reactor temperature would be necessary in order to achieve complete conversion of the fuel. Hence it would be very interesting to carry out chemical-looping reforming experiments at elevated pressure.

7. Conclusions

Three NiO based oxygen-carrier materials for chemical-looping applications have been tested. N2AM1400 was produced by freeze granulation, while Ni18-αAl and Ni21-γAl and were produced by impregnation. Over 160 hours of continuously operating experiments in a small circulating fluidized-bed reactor have been recorded.

The conversion of natural gas into reagents was very high for all three materials. For chemical-looping combustion experiments, there was no or barely measurable amounts of CH_4 in the fuel reactor gas, at any temperature in the examined span of 800-950 ºC. For chemical-looping reforming experiments, the conversion of CH_4 into reagents was 96-100%, depending on temperature, oxygen carrier and experimental conditions. Typically, there was no measurable CH_4 in the outlet gas if the fuel reactor temperature was 930ºC or above.

The gas composition after the fuel reactor was reasonably close to thermodynamical equilibrium for the water-gas shift reaction. For N2AM1400 the H_2 concentration was 2-3% points below equilibrium though.

When only natural gas was used as fuel, there was formation of solid carbon on Ni18-αAl and Ni21-γAl. This was true not only for chemical-looping reforming, but for chemical-looping combustion as well, which was unexpected.

High fuel reactor temperature was beneficial both for combustion and reforming applications. For combustion, increased fuel-reactor temperature resulted in increased CO_2 yield. For reforming applications, increased fuel-reactor temperature resulted in increased conversion of natural gas and seemingly also reduced formation of solid carbon in the fuel reactor.

For chemical-looping reforming, operating the reactor at the desired process parameters of T_{FR}=950ºC and Ψ=0.30-0.35 with 30% steam added to the natural gas was possible with all of the three tested oxygen-carrier materials. It was possible to substitute the steam for CO_2 and still have a smooth running process with no or very small formation of solid carbon. This verifies that chemical-looping reforming is a feasible concept for production of synthesis gas and H_2.

For chemical-looping combustion, Ni21-γAl provided poor selectivity towards CO_2 and is probably not suitable for chemical-looping combustion. N2AM1400 was slightly better, but highly sensitive to the temperature in the fuel reactor. Ni18-αAl initially provided excellent results, but after a few hours of operation the selectivity towards CO_2 had declined significantly. Ni21-γAl and Ni18-αAl also propagated carbon formation in the fuel reactor, unless some H_2O or CO_2 was added to the fuel. All three tested oxygen carriers showed lower

conversion to CO_2 compared to NiO-based materials previously examined by Johansson et al [9, 18]. The NiO content of these previously tested oxygen carriers were much higher compared to those examined here though.

N2AM1400 and Ni18-αAl seem to have retained their physical and chemical structure well over the course of the experiments. Ni21-γAl displayed a reduction in porosity, but remained highly reactive. Despite the sometimes harsh experimental conditions, the experiments ran perfectly smooth and there were no signs of agglomeration or defluidization for any of the oxygen-carrier materials.

8. Acknowledgements

The authors wish to thank our financers, supporters and co-workers within the CACHET project, contract 019972 under the 6th framework programme funded by the European Commission. A special thanks to our colleagues at CSIC-ICP in Zaragoza, who manufactured the Ni18-αAl and Ni21-γAl oxygen carriers.

9. References

(1) Cho, P. *Development and characterization of oxygen-carrier materials for chemical-looping combustion*. Chalmers University of Technology: Göteborg, Sweden, 2005.

(2) Johansson, M. *Screening of oxygen-carrier particles based on iron-, manganese-, copper-and nickel oxides for use in chemical-looping technologies*. Chalmers University of Technology: Göteborg, Sweden, 2007.

(3) Adánez, J.; de Diego, L. F.; García-Labiano, F.; Gayán, P.; Abad, A. *Energy & Fuels* **2003**, 18, 371-377.

(4) Jerndal, E.; Mattisson, T.; Lyngfelt, A. *Chemical Engineering Research and Design* **2006**, 84, 795-806.

(5) Cho, P.; Mattisson, T.; Lyngfelt, A. *Industrial & Engineering Chemistry Research* **2005**, 44, 668-676.

(6) Lyngfelt, A.; Kronberger, B.; Adánez, J.; Morin, J. X.; Hurst, P. The GRACE project. Development of oxygen carrier particles for chemical-looping combustion. Design and operation of a 10 kW chemical-looping combustor. *Proceedings of the 7th International Conference on Greenhouse Gas Control Technologies* (Vancouver, Canada, 2004).

(7) Ryu, H. J.; Jin, G. T.; Yi, C. K. Demonstration of inherent CO_2 separation and no NO_X emission in a 50 kW chemical-looping combustor - continuous reduction and oxidation experiment. *Poster presented at the 7th International Conference on Greenhouse Gas Control Technologies* (Vancouver, Canada, 2004).

(8) Johansson, E.; Mattisson, T.; Lyngfelt, A.; Thunman, H. *Chemical Engineering Research and Design* **2006**, 84, 819-827.

(9) Johansson, E.; Mattisson, T.; Lyngfelt, A.; Thunman, H. *Fuel* **2006**, 85, 1428-1238.

(10) Abad, A.; Mattisson, T.; Lyngfelt, A.; Rydén, M. *Fuel* **2006**, 85, 1174-1185.

(11) Abad, A.; Mattisson, T.; Lyngfelt, A.; Johansson, M. *Fuel* **2007**, 86, , 1021-1035.

(12) Adánez, J.; Gayán, P.; Celaya, J.; de Diego L.; García-Labiano, F.; Abad, A. *Industrial & Engineering Chemistry Research* **2006**, 45, 6075-6080.

(13) Linderholm, C.; Abad, A.; Mattisson, T.; Lyngfelt, A. *160 hours of chemical-looping combustion in a 10 kW reactor system with a NiO-based oxygen carrier*. Accepted for publication in International Journal of Greenhouse Gas Control 2008.

(14) de Diego, L.; García-Labiano, F.; Gayán, P.; Adánez, J.; Celaya, J.; Palacios, J. M. *Fuel* **2007**, 86, 1036-1045.

(15) Abad, A.; García-Labiano, F.; de Diego, L.; Gayán, P.; Adánez, J. *Energy & Fuels* **2007**, 21, 1843-1853.

(16) Abad, A.; Adánez, J.; García-Labiano, F.; de Diego, L.; Gayán, P.; Celaya, J. *Chemical Engineering Science* **2007**, 62, 533-549.

(17) García-Labiano, F.; de Diego, L.; Gayán, P.; Adánez, J.; Abad, A. Energy & Fuels **2006**, 20, 26-33.

(18) Brandvoll, Ø. *Chemical looping combustion: fuel conversion with inherent CO_2 capture.* Norwegian University of Science and Technology: Trondheim, Norway, 2005.

(19) Johansson, E. *Fluidized-bed reactor systems for chemical-looping combustion with inherent CO_2 capture*. Chalmers University of Technology: Göteborg, Sweden, 2005.

(20) Wolf, J. *CO_2 mitigation in advanced power cycles.* The Royal Institute of Technology: Stockholm, Sweden, 2004.

(21) Kronberger, B. *Modelling analysis of fluidised bed reactor systems for chemical-looping combustion.* Vienna University of Technology: Vienna, Austria, 2005.

(22) Naqvi, R. *Analysis of gas-fired power cycles with chemical looping combustion for CO_2 capture.* Norwegian University of Science and Technology: Trondheim, Norway, 2006.

(23) Mattisson, T.; Lyngfelt, A. Applications of chemical-looping combustion with capture of CO_2. *Proceedings of the 2th Nordic Minisymposium on Carbon Dioxide Capture and Storage* (Göteborg, Sweden, 2001).

(24) Arnold, C. *Process for production of carbon monoxide and hydrogen.* Patent specification 636,206, The Patent Office, London, United Kingdom, 1950.

(25) Zafar, Q.; Mattisson, T.; Gevert, B. *Industrial & Engineering Chemistry Research* **2005**, 44, 3485-3498.

(26) Mattisson, T.; Zafar, Q.; Lyngfelt, A.; Gevert, B. *Integrated hydrogen and power production from natural gas with CO_2 capture.* Proceedings of the 15th World Hydrogen Energy Conference (Yokohama, Japan, 2004).

(27) Rydén, M.; Lyngfelt, A.; Mattisson, T. *Fuel* **2006**, 85, 1631-1641.

(28) Rydén, M. *Hydrogen production with carbon dioxide capture by reforming of natural gas using chemical-looping technologies.* Chalmers University of Technology: Göteborg, Sweden, 2006.

(29) Stobbe, E. R.; De Boer, B. A.; Geus J. W. *Catalysis Today* **1999**, 47, 161-167.

(30) Fathi, M.; Bjørgum, E.; Viig, T.; Rokstad, O. A. *Catalysis Today* **2000**, 63, 489-497.

(31) Gavalas, G. R.; Kim, K.; Pantu, O. *Applied Catalysis A: General* **2000**, 193, 203-214.

(32) Jalibert, J. C.; Fathi, M.; Rokstad, O. A.; Holmen, A. *Studies in Surface Science and Catalysis* **2001**, 136, 301-306.

(33) Shen, S. K.; Yu, C. C.; Li, R J. *Journal of Natural Gas Chemistry* **2002**, 11, 137-144.

(34) Shen, S. K.; Yu, C. C.; Li, R J. *Studies in Surface Science and Catalysis* **2004**, 147, 139-144.

(35) Zeng, Y.; Tamhankar, S.; Ramprasad, N.; Fitch, F.; Acharya, D.; Wolf, R. *Chemical Engineering Science* **2003**, 58, 577-582.

(36) Li, R.; Yu, C.; Zhu, G.; Shen, S. *Petroleum Science* **2005**, 2, 19-23.

(37) Bjørgum, E. *Methane conversion over mixed metal oxides.* Norwegian University of Science and Technology: Trondheim, Norway, 2005.

(38) Rydén, M.; Lyngfelt, A.; Mattisson, T.; Chen, D.; Holmen, A.; Bjørgum, E. *International Journal of Greenhouse Gas Control* **2008**, 2, p 21-36.

(39) Rydén, M.; Lyngfelt, A. Hydrogen and power production with integrated carbon dioxide capture by chemical-looping reforming. *Proceedings of the 7th International Conference on Greenhouse Gas Control Technologies* (Vancouver, Canada, 2004).

Abbreviations

CLC	Chemical-looping combustion
CLR	Chemical-looping reforming
$CLR_{(ng)}$	CLR experiment with natural gas as fuel
$CLR_{(H2O)}$	CLR experiment with natural gas mixed with steam as fuel
$CLR_{(CO2)}$	CLR experiment with natural gas mixed with CO_2 as fuel
m	Mass
Me	Generic oxygen carrier, reduced
MeO	Generic oxygen carrier, oxidized
C_nH_m	Generic hydrocarbon fuel
L_n/min	Normal litres per minute
x_i	Dry-gas molar ratio of component i
y_i	Wet-gas molar ratio of component i
F_i	Volumetric flow of component i,
Ψ	Degree of oxidation of fuel-reactor gas
γ_{CO2}	CO_2 yield
$F_{fr \rightarrow ar}$	Gas leakage from fuel reactor to air reactor
ρ	Density
K(T)	Equilibrium constant for the water-gas shift reaction
(H/C)	Hydrogen to carbon ratio
(O/C)	Oxygen to carbon ratio
C_{ar}/C_{tot}	Total carbon leakage to the air reactor
C/C_{tot}	Carbon formation
C_{ack}/C_{tot}	Carbon accumulation

Indexes

ng	Natural gas
oc	Oxygen carrier
air	Air
fr	Fuel reactor
ar	Air reactor
fm	Fuel mix
cc	Complete combustion
eq	Equilibrium
dry	Dry gas